Journal of The Electrochemical Society

Zirconium Oxide-Based Compound as New Cathode Without Platinum Group Metals for PEFC

Journal of The Electrochemical Society, **157** (6) B885-B891 (2010)
0013-4651/2010/157(6)/B885/7/$28.00 © The Electrochemical Society

Zirconium Oxide-Based Compound as New Cathode Without Platinum Group Metals for PEFC

Y. Ohgi, A. Ishihara,* K. Matsuzawa,* S. Mitsushima,* and K. Ota*,z

Chemical Energy Laboratory, Yokohama National University, Yokohama 240-8501, Japan

Partially oxidized zirconium carbonitride (Zr-CNO) powders were evaluated as a nonprecious metal cathode for polymer electrolyte fuel cells (PEFCs). Zr-CNO powders were prepared from zirconium carbonitrides ($ZrC_{0.5}N_{0.5}$) with heat-treatment under N_2 containing 2% H_2 and 0.25% O_2 gas at 1000–1400°C. Voltammetry was performed to evaluate the catalytic activity for oxygen reduction reaction (ORR) under nitrogen and oxygen in 0.1 mol dm^{-3} H_2SO_4 at 30°C. Although the onset potential of the ORR for untreated $ZrC_{0.5}N_{0.5}$ was 0.55 V vs a reversible hydrogen electrode (RHE), the onset potential of the appropriate oxidized Zr-CNO reached 0.97 V vs RHE. X-ray diffraction and X-ray photoelectron spectroscopy data suggested that the surface of Zr-CNO was oxidized to ZrO_2, and $ZrC_{0.5}N_{0.5}$ remained in the inner part of the Zr-CNO particles.
 [DOI: 10.1149/1.3382960]

Manuscript submitted October 1, 2009; revised manuscript received January 21, 2010. Published April 27, 2010.

Polymer electrolyte fuel cells (PEFCs) are expected to become a prominent technology in a variety of energy generation applications such as residential, portable, and automotive power sources due to their high efficiency of energy conversion, low pollutant emission, and high power density. There are, however, some technological and economical problems before the widespread commercialization. One of the big technological problems is a large overpotential of the oxygen reduction reaction (ORR), although platinum is utilized as an electrocatalyst in the present systems. The large overpotential of the ORR should be reduced to obtain high energy efficiency. The biggest economical problem is the high cost of platinum catalysts due to the limitation of its amount of resources. Although many attempts have been made to reduce platinum usage, the cost of electrodes remains high. Therefore, the development of a nonprecious metal-based catalyst is strongly required.

Many studies have been performed to develop nonplatinum cathode catalysts for low temperature fuel cells. Macrocyclic transition-metal (cobalt or iron mainly acted as an active site) complexes and novel metal chalcogenides were famous as candidates for an alternative platinum catalyst. Since the early 1960s, transition-metal complexes of the N_4-chelate type, such as phthalocyanines, porphyrins, and tetraazaanulens, had some catalytic activity for the ORR.[1-3] However, these compounds were unstable in an acidic and oxidizing atmosphere.[4] In recent years, heat-treatment of the carbon-supported N_4-chelates containing iron and cobalt was found to greatly enhance catalytic activity and stability.[5] However, the stability of the complexes is still insufficient because the PEFC cathode is a severe corrosive atmosphere.

Alonso-Vante and co-workers reported chalcogenide clusterlike materials such as $Mo_xRu_ySe_z$ [6,7] and Ru_xX_y (where X = S, Se, and Te)[8,9] as nonplatinum cathodes. These chalcogenides exhibited enhanced activity toward selective ORR with methanol-tolerant characteristics in acid in the presence of methanol.[10-12] The clusterlike Ru_xSe_y compounds had a ruthenium atom as a core, and selenium is probably coordinated at the surface of ruthenium nanoparticles. The role of Se was proposed to chemically stabilize the metallic Ru centers against oxidation.[8,13] However, selenium was oxidized and dissolved readily in acid, and it disappeared on the surface.[9] Consequently, these catalysts have a poor long-term stability in acid.

It is believed that a high stability is essentially required because the cathode catalysts are exposed to an acidic and oxidizing atmosphere, namely, a strong corrosive environment. We paid attention to the high stability of groups IV and V metal oxides, which are well known as valve metals. However, groups IV and V metal oxides are generally insulators so that these oxides have a large bandgap and the redox reaction hardly occurs on the surface of the oxides. Therefore, the surface of the oxides must be modified for the ORR to proceed on the surface. In recent years, our research group has reported that oxide-based transition-metal compounds such as titanium oxide,[14] titanium oxynitride,[15] tantalum oxynitride,[16-18] tantalum oxycarbonitride,[19,20] zirconium oxide,[21] and zirconium oxynitride[22-24] were stable in an acid solution and had some catalytic activity for the ORR. The surface of these compounds was modified with defects of oxygen and doping of nitrogen. In particular, partially oxidized tantalum carbonitride (Ta-CN) powder had a high catalytic activity for the ORR.[21,22] Although partially oxidized Ta-CN would be one of the possible candidates as a nonplatinum cathode, the resource of tantalum is as small as that of platinum. However, the resource of zirconium oxide, 51×10^3 kton, is 3 orders of magnitude greater than that of platinum (39 kton). Zirconium oxides might be a good candidate for the nonprecious metal cathode of PEFCs, considering the stability and the amount of resources.

In this paper, Zr-CNs (expressed as $ZrC_{0.5}N_{0.5}$) were used as starting materials, and a partial oxidation of $ZrC_{0.5}N_{0.5}$ was performed to obtain a zirconium oxide-based compound with control of the oxidation state. Physical and chemical properties of zirconium oxide strongly depended on the crystalline structure. ZrO_2 has three stable crystalline structures such as monoclinic, tetragonal, and cubic. Monoclinic ZrO_2 is thermochemically stable at room temperature under ambient pressure. However, the other crystalline structure can exist stably at room temperature under ambient pressure by increasing the concentration of oxygen defect and nitrogen atoms.[25,26] Oxygen defects and doping of nitrogen atom on the surface might act as active sites of the ORR. In this paper, the zirconium oxide-based compound prepared by the partial oxidation of $ZrC_{0.5}N_{0.5}$ is evaluated as a nonprecious metal cathode for PEFCs, and the correlation between the physicochemical properties and the catalytic activity for the ORR is discussed.

Experimental

Synthesis of electrocatalysts.— Carbon powders of the amount according to the stoichiometric ratio of Eq. 1 were mixed with zirconium oxide, and the mixture was heated at 1800°C under nitrogen atmosphere to synthesize Zr-CN as a starting material

$$ZrO_2 + 2.5C \rightarrow ZrC_{0.5}N_{0.5} + 2CO \quad [1]$$

The carbon content of Zr-CN was determined with an IR absorption method after combustion by high frequency induction using a high frequency IR carbon–sulfur analyzer instrument (CS-600 series, LECO Japan Co., Japan). The nitrogen and oxygen contents of Zr-CN were determined using the inert-gas fusion thermal conductivity method and the inert-gas fusion IR absorption method (TCH600 series, LECO Japan Co., Japan), respectively. The overall chemical composition of Zr-CN was determined to be $ZrC_{0.5}N_{0.5}$.

Partial oxidation was performed with the heat-treatment of the $ZrC_{0.5}N_{0.5}$ powders at 1000, 1200, and 1400°C for 10 h under N_2

* Electrochemical Society Active Member.
z E-mail: ken-ota@ynu.ac.jp

containing 2% H_2 and 0.25% O_2 gas at a flow rate of 15 cm^3 min^{-1} in an alumina tube furnace (KT-3 × 14-VP, Koyo Thermo Systems, Japan) to prepare partially oxidized zirconium carbonitride (Zr-CNO) powders. Although the oxidation of Zr-CN was the purpose, the reason for adding hydrogen into the heat-treatment atmosphere was that an addition of hydrogen caused Zr-CN to oxidize uniformly. In addition, Zr-CNO heat-treated at 1000°C for 15 h at a flow rate of 15 cm^3 min^{-1} was prepared to evaluate the effect of the mixing ratio of Ketjen Black (KB) EC 300J as a current collector on the potential–current curve for the ORR.

Electrochemical measurements.— A partially oxidized $ZrC_{0.5}N_{0.5}$ (Zr-CNO) had poor electrical conductivity because the surface was considerably oxidized. A mixture of partially oxidized CN with KB as the current collector was very useful to obtain a large ORR current.[20] First, the effect of mixing ratio of KB EC 300J to Zr-CNO on the potential–current curve for the ORR was examined using Zr-CNO heat-treated at 1000°C for 15 h under N_2 containing 2% H_2 and 0.25% O_2 gas at a flow rate of 15 cm^3 min^{-1}. A suitable mixing ratio of KB to Zr-CNO was selected. The mixed powder of 30 mg was dispersed in 1.0 cm^3 of distilled water to make the catalyst ink. The ink was dropped on a glassy carbon (GC) rod (5.2 mm diameter, Tokai Carbon Co., Japan) with Zr-CNO mixed with KB of ca. 2 mg and covered with 0.5 wt % recast Nafion solution. This ink was also used for the fabrication of a rotating ring-disk electrode (RRDE), as we describe below. All electrochemical experiments were conducted with a three-electrode cell under oxygen or nitrogen atmosphere in 0.1 M (M: mol dm^{-3}) H_2SO_4 at 30°C using a PS08 potentiostat (TOHO Technical Research, Japan). A reversible hydrogen electrode (RHE) and a GC plate were used as reference and counter electrodes, respectively. Before the evaluation of the catalytic activity and the stability, cyclic voltammetry under oxygen was carried out at a scan rate of 50 mV s^{-1} from 0.05 to 1.2 V in 0.1 M H_2SO_4 at 30°C to clean up the surface until the cyclic voltammogram (CV) reached a steady state. Then, the catalytic activity for the ORR was determined by voltammetry at a sweep rate of 5 mV s^{-1} under oxygen and nitrogen from 1.2 to 0.2 V. A current difference between under oxygen and under nitrogen would be due to the oxygen reduction, that is, the ORR current (i_{ORR}). The onset potential for the ORR was defined as the electrode potential at $i_{ORR} = -0.2$ μA cm^{-2}. After determining the ORR activity, the electrochemical stability was evaluated by cyclic voltammetry at a sweep rate of 5 mV s^{-1} under nitrogen from 0.05 to 1.2 V in 0.1 M H_2SO_4 at 30°C. To examine the durability of the catalysts, the working electrode was prepared using the catalyst ink, which was stored in a glass bottle for 8 months at room temperature under atmosphere, and the catalytic activity was measured. A current density was based on the geometric surface area of the working electrode.

H_2O_2 generation of the zirconium-based catalysts in the ORR was investigated using the RRDE technique. The RRDE measurements were performed with a rotor (Nikko Keisoku, Japan) and a PS08 potentiostat. The RRDE was an assembly made of a zirconium-based catalyst powder-coated GC disk (6 mm diameter) mounted in a poly(tetrafluoroethylene) holder, which was surrounded by a Pt ring (inner diameter: 7 mm and outer diameter: 9 mm). The same catalyst ink was dropped on the GC disk electrode with Zr-CNO mixed with KB of ca. 2 mg on GC (6 mm diameter) and covered with 0.5 wt % recast Nafion solution. The electrochemical measurements were carried out using a three-electrode cell under O_2 or N_2 atmosphere in 0.1 M H_2SO_4 at 30°C. RHE and a GC plate were also used as reference and counter electrodes, respectively.

The catalyst-coated GC disks were electrochemically cleaned by sweeping the potential from 0.2 to 1.0 V at a sweep rate of 50 mV s^{-1} under N_2 for 100 potential cycles. For ORR studies, voltammogram was recorded from 1.2 to 0.2 V at 5 mV s^{-1} with the rotation speed of the electrode at 400–3600 rpm under oxygen and nitrogen.

To oxidize any H_2O_2 that was generated during the progress of the ORR at the disk, the ring potential was held at 1.1 V. The % H_2O_2 produced was determined with the following equation[27]

$$\%\ H_2O_2 = 100 \times (2I_R/N)/[I_D + (I_R/N)] \quad [2]$$

where I_D is the faradaic current at the disk, I_R is the faradaic current at the ring, and N is the RRDE collection efficiency. Based on the geometry of the electrodes and their dimensions, the collection efficiency was theoretically calculated to be 0.345. The collection efficiency (N) of the ring electrode was experimentally determined by the reduction and oxidation of ferrocyanide ions at the disk and ring electrodes, respectively. The collection efficiency was obtained from the ratio of ring to disk currents: $N = -I_{ring}/I_{disk}$. In this study, the RRDE collection efficiency N was experimentally estimated to be 0.32, and this value was used as N.

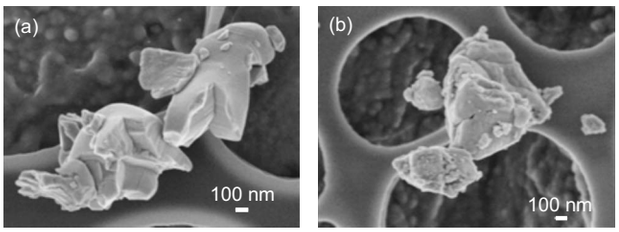

Figure 1. SEM images of (a) Zr-CN, Zr-CNO with heat-treatment at (b) 1200°C.

Characterization.— The crystalline structure of the specimens was characterized using an X-ray diffractometer (XRD, XRD-6000, Shimadzu, Japan) with Cu Kα in the range from 15 to 85° to confirm the partial oxidation. $ZrC_{0.5}N_{0.5}$ powders with and without heat-treatment were directly observed using a scanning electron microscope (SEM, JSM-7500F, JEOL, Japan) at an accelerating voltage of 10 kV. X-ray photoelectron spectroscopy (AXIS-NOVA, Kratos) was performed to investigate the chemical bonding state of the surface of the specimens at an accelerating voltage of 10 kV. The peak of the C–C bond attributed to free carbon at 284.6 eV in the C 1s spectrum was used to compensate for surface charging in X-ray photoelectron spectroscopy (XPS).

Results and Discussion

Surface morphology.— SEM images of the starting material, $ZrC_{0.5}N_{0.5}$, and Zr-CNO prepared at 1200°C are shown in Fig. 1. The particle sizes of $ZrC_{0.5}N_{0.5}$ and Zr-CNO were of the micrometer or submicrometer order. The surface of Zr-CNO prepared at 1200°C was rougher than that of $ZrC_{0.5}N_{0.5}$, and submicrometer holes existed on the surface of Zr-CNO. In addition, the particle size of Zr-CNO prepared at 1200°C was smaller than that of $ZrC_{0.5}N_{0.5}$. The same phenomena for the other Zr-CNO treated at 1000 and 1400°C occurred with partial oxidation. Shimada et al. revealed that N_2 gas evolved in advance of CO_2 gas in the early stage of oxidation of the CNs.[28] During the heat-treatment, $ZrC_{0.5}N_{0.5}$ would be oxidized to produce gases such as CO_2 and N_2

$$ZrC_xN_{1-x} + (1 + x)O_2 \rightarrow ZrO_2 + xCO_2 + (1 - x)N_2 \quad [3]$$

These produced gases might cause the formation of submicrometer holes on the surface. Therefore, the surface area of Zr-CNO probably became larger than that of $ZrC_{0.5}N_{0.5}$.

Progress of partial oxidation.— Figure 2 illustrates the XRD patterns of the starting material, $ZrC_{0.5}N_{0.5}$, Zr-CNO with heat-treatment at 1000, 1200, and 1400°C and commercial zirconia (Wako Pure Chemicals Co., Japan). An expanded view from ca. 28 to 32° is also shown because the maximum and second maximum peaks of monoclinic, tetragonal, and cubic ZrO_2 exist in the range from ca. 28 to 32°. The intensity of each XRD pattern was normalized relative to the maximum value.

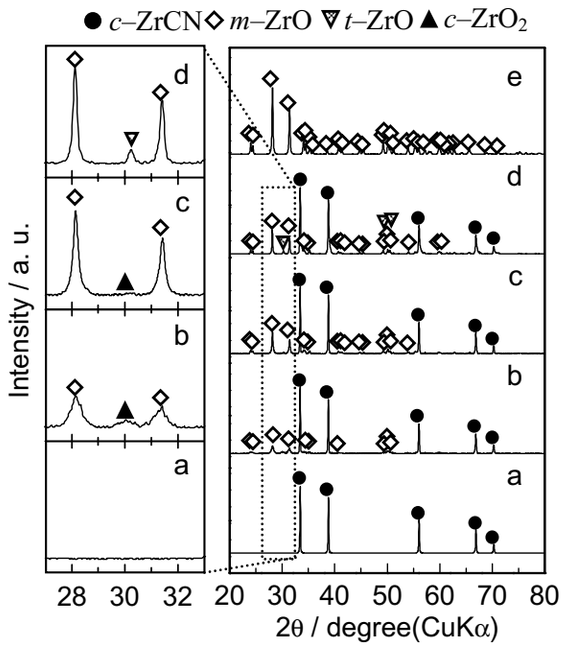

Figure 2. XRD patterns of (a) Zr-CN, Zr-CNO with heat-treatment at (b) 1000, (c) 1200, and (d) 1400°C, and (e) ZrO_2.

Both ZrC and ZrN have the same crystalline structure (rock-salt type) and form a complete solid solution. The peak pattern does not change from ZrC (JCPDS 35-0784) to ZrN (JCPDS 35-0753), and each peak shifts to a higher angle with the increase in nitrogen content, which is known as Vegard's law. In this paper, the compounds with XRD peaks that existed between ZrC and ZrN were expressed as ZrC_xN_y. The surface of the starting material, $ZrC_{0.5}N_{0.5}$, was probably oxidized in air because no peaks due to oxide were observed. The surface oxide layer of $ZrC_{0.5}N_{0.5}$ might be very thin. The peak intensity of monoclinic ZrO_2 increased, and the peak intensity of ZrC_xN_y decreased with increasing heat-treatment temperature. Therefore, it was confirmed that the partial oxidation proceeded during the heat-treatment because the flowing gas contains oxygen.

The color of the powder turned from deep purple, which was due to $ZrC_{0.5}N_{0.5}$, to black through the heat-treatment. In addition, the peaks that belong to tetragonal and cubic ZrO_2 around 30° were also observed in the patterns of all Zr-CNOs, as shown in Fig. 2b-d.

Electrochemical stability.— Sufficient stability, as well as high catalytic activity toward the ORR, is essential for nonprecious metal cathodes for PEFCs. Even if the catalytic activity of nonprecious cathodes is almost similar to that of Pt, the ORR activity of the specimen with insufficient stability would deteriorate during the long-term operation. Figure 3 shows the steady-state CV of $ZrC_{0.5}N_{0.5}$, Zr-CNO prepared at 1000, 1200, and 1400°C and ZrO_2 mixed with KB of 5 wt % in 0.1 M H_2SO_4 at 30°C under N_2. The CV of $ZrC_{0.5}N_{0.5}$ was smaller than those of Zr-CNO powders and ZrO_2, reflecting that the surface area of Zr-CNO probably increased due to partial oxidation. The shape of the CVs was almost the same. When redox reactions, such as metal dissolution into acidic media, occur on the test electrode in an acidic solution, some specific peaks are observed. In fact, the reversible peak at around 0.4–0.6 V might be responsible for the redox reaction due to surface functional groups such as quinone and hydroquinone adsorbed on carbon black.[29] Thus, there were no specific peaks resulting from the degradation of the Zr-based catalysts except the redox peaks due to the surface functional group on KB in all CV of Zr-CNO. Therefore, Zr-CNO prepared at 1000, 1200, and 1400°C would be electrochemically stable in acidic media.

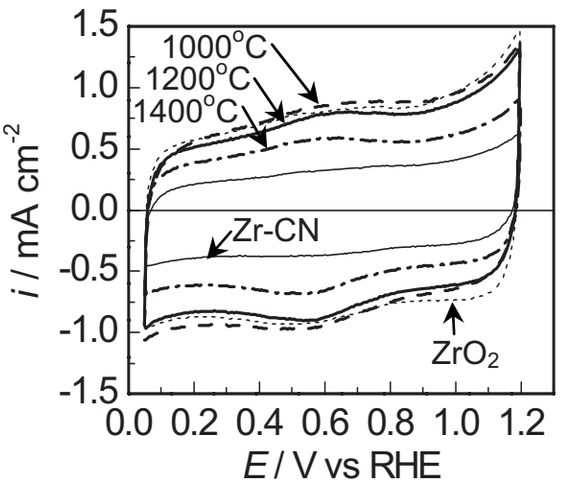

Figure 3. Steady-state CV of Zr-CN, Zr-CNO with heat-treatment at 1000–1400°C, and ZrO_2 in 0.1 M H_2SO_4 at 30°C under N_2.

ORR activity.— Figure 4 shows the effect of the mixing ratio of KB on the potential–current curves of Zr-CNO heat-treated at 1000°C for 15 h under N_2 containing 2% H_2 and 0.25% O_2 gas at a flow rate of 15 cm^3 min^{-1}. An increase in the mixing ratio of KB from 3 to 8 wt % brought the increase in the current due to the charge/discharge of the electrical double layer. The difference in the current density between under N_2 and under O_2 with a mixing ratio of KB of 8 wt % was larger than that with a mixing ratio of KB of 3 wt %. The difference in the current density between under N_2 and under O_2 was responsible for the ORR. Therefore, this result indicates that the mixing ratio of KB strongly affected the i_{ORR} current.

Figure 5 shows the dependence of the onset potential for the ORR (E_{ORR}) on the mixing ratio of KB. The E_{ORR} increased up to ca. 5 wt % and decreased above 8 wt %. The increase in E_{ORR} was probably due to the improvement of the electric conductivity of the catalyst because of the addition of KB. However, if KB only acted as a current collector, the E_{ORR} might be constant above a certain mixing ratio of KB. Therefore, the decrease above 8 wt % suggested that there might exist some specific interactions between Zr-CNO

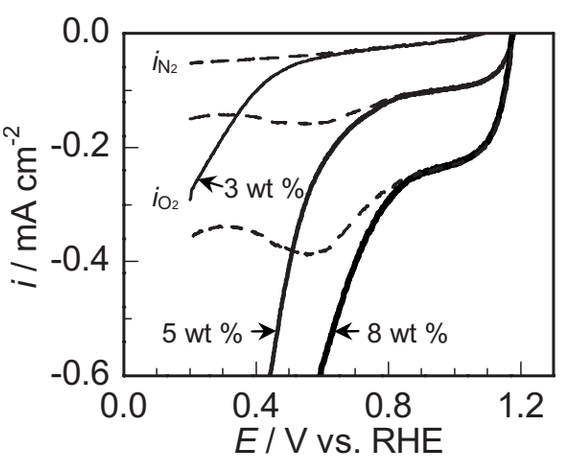

Figure 4. Effect of the mixing ratio of KB on the potential–current curves of Zr-CNO heat-treated at 1000°C for 15 h at a flow rate of 15 mL min^{-1} under O_2 (solid lines) and N_2 (dashed lines) atmospheres.

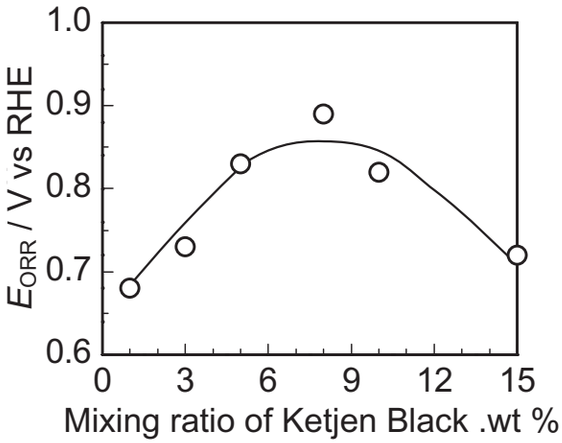

Figure 5. Dependence of onset potential for the ORR on mixing ratio of KB.

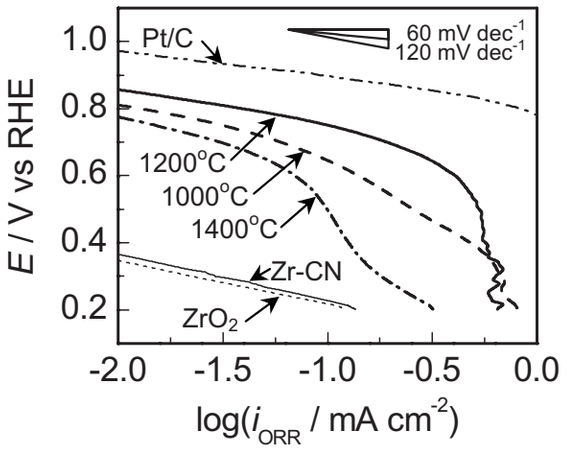

Figure 7. Tafel plots for i_{ORR} on Zr-CN, Zr-CNO with heat-treatment at 1000–1400°C, ZrO_2, and 46.3 wt % Pt/C. Pt loading: 3 μg/GC rod (ϕ5.2 mm).

and KB. Although the specific interaction between Zr-CNO and KB was important for making a catalyst layer of the actual cell, the mixing ratio of KB was fixed at 5 wt % to compare the catalytic activity of Zr-CNO in this paper.

Figure 6 shows the potential–current curves for the ORR on $ZrC_{0.5}N_{0.5}$, Zr-CNO prepared at 1000, 1200, and 1400°C and commercial ZrO_2 in 0.1 M H_2SO_4 at 30°C. A potential–current curve of 46.3 wt % Pt/C (Tanaka Kikinzoku Kogyo, Japan) is also plotted for comparison. The ORR current density of Pt/C was based on the geometrical surface area of GC rod, and the Pt loading was 3.0 μg/GC rod (ϕ5.2 mm), that is, 14 μg cm^{-2} geometric area. The ORR current of $ZrC_{0.5}N_{0.5}$ and ZrO_2 was observed below 0.5 V, indicating that $ZrC_{0.5}N_{0.5}$ and ZrO_2 had poor catalytic activity toward the ORR. However, the ORR current of Zr-CNO prepared at 1000, 1200, and 1400°C was clearly observed at a higher potential. In particular, Zr-CNO prepared at 1200°C shows the highest catalytic activity, and its onset potential reached 0.97 V vs RHE. Therefore, the partial oxidation of $ZrC_{0.5}N_{0.5}$ was greatly useful to enhance the catalytic activity for the ORR. The onset potential of Pt/C was 1.05 V, which was about 0.1 V higher than that of Zr-CNO prepared at 1200°C, and the catalyst loading of Zr-CNO was much greater than that of Pt/C. The catalytic activity of Zr-CNO for the ORR would not get the activity of Pt/C. However, because Zr has abundant amounts of the resource and the onset potential reached 0.97 V, the partially oxidized $ZrC_{0.5}N_{0.5}$ might have a potential of an alternative cathode of nonprecious metal for PEFCs.

Figure 7 shows Tafel plots for the ORR on $ZrC_{0.5}N_{0.5}$, Zr-CNO with heat-treatment at 1000–1400°C, ZrO_2, and 46.3 wt % Pt/C. The Tafel slope of Pt/C in the current density range from 10^{-2} to 10^{-1} mA cm^{-2} was ca. 73 mV dec^{-1}. As shown in Fig. 7, Zr-CNO with heat-treatment at 1000–1400°C had similar Tafel slopes in the high potential region. However, the Tafel slope of $ZrC_{0.5}N_{0.5}$ and ZrO_2 was larger than that of Zr-CNO. Because $ZrC_{0.5}N_{0.5}$ and ZrO_2 had a low catalytic activity, the ORR current started to flow below 0.5 V. Below 0.5 V, KB acted as a catalyst that reduced oxygen to hydrogen peroxide. The complex of reactions affected the Tafel slope of $ZrC_{0.5}N_{0.5}$ and ZrO_2.

The long-term storage test for the catalytic activity was conducted with the most active Zr-CNO, which was prepared at 1200°C. The catalyst ink, which was used to prepare the working electrode, was stored in a glass bottle for 8 months at room temperature. The working electrode was prepared again using the stored catalyst ink, and a voltammetry at 5 mV s^{-1} was performed. Figure 8 shows the Tafel plots for the ORR of the Zr-CNO prepared at 1200°C before and after ink storage. As shown in Fig. 8, their Tafel plots were nearly the same, although a slight decrease was observed

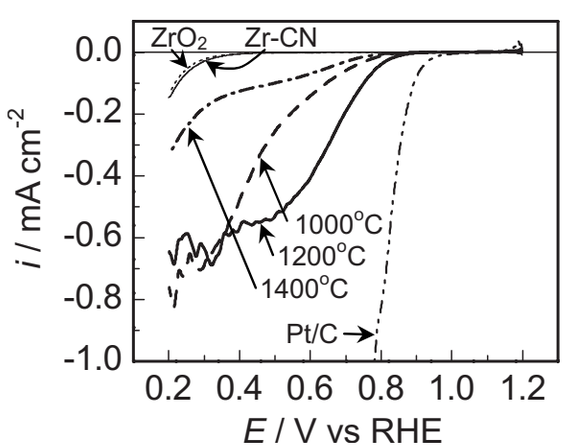

Figure 6. Potential–current (i_{ORR}) curves for the ORR on Zr-CN, Zr-CNO with heat-treatment at 1000–1400°C, ZrO_2, and 46.3 wt % Pt/C at 5 mV s^{-1} in 0.1 M H_2SO_4 at 30°C. Pt loading: 3 μg/GC rod (ϕ5.2 mm).

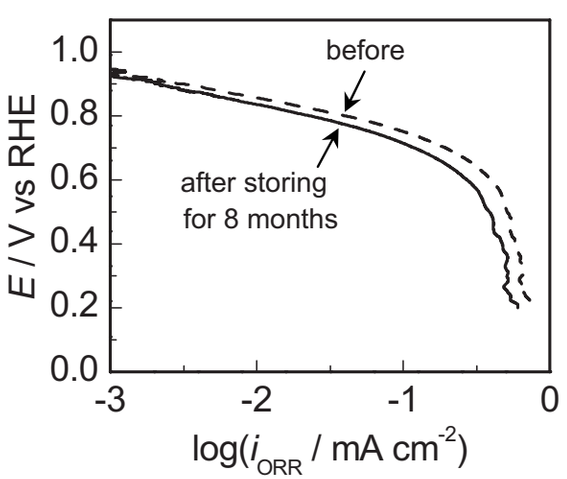

Figure 8. Tafel plots for the ORR on Zr-CNO with heat-treatment at 1200°C (loading: 7.5 mg cm^{-2}) (dashed lines) and the same specimen preserved in ink for 8 months (loading: 9.1 mg cm^{-2}) (solid lines).

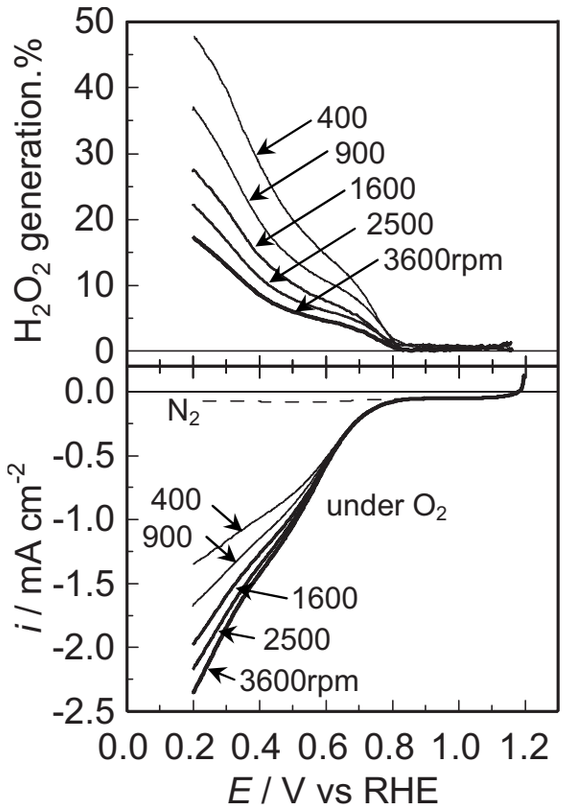

Figure 9. Polarization curves at 400–3600 rpm as a function of the disk potentials and the H_2O_2 generation at the ring for ORR catalyzed by Zr-CNO treated at 1200°C. Pt ring held at 1.1 V vs RHE.

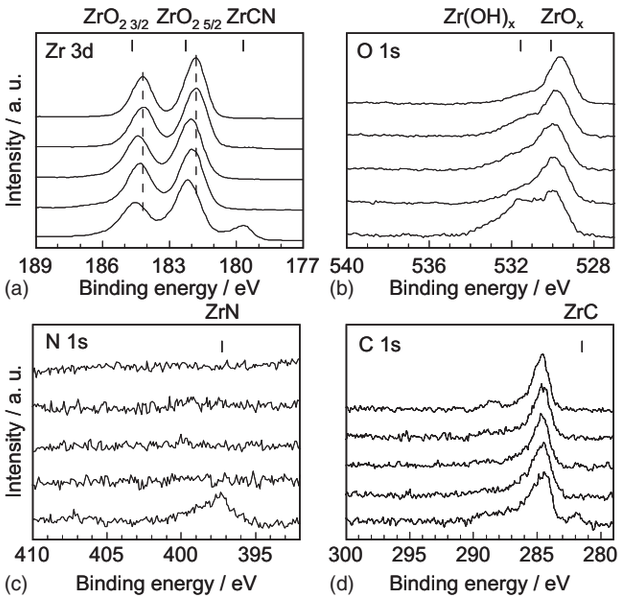

Figure 10. XPS Zr 3d, O 1s, N 1s, and C 1s spectra of (a) Zr-CN, Zr-CNO with heat-treatment at (b) 1000, (c) 1200, and (d) 1400°C, and (e) ZrO_2.

in Zr-CNO prepared using the catalyst ink that was stored for 8 months. This result revealed that the catalytic activity of Zr-CNO was maintained after the catalyst was immersed in distilled water for 8 months. Therefore, the surface state of Zr-CNO, including the active site, was stable for a long time. The high stability of the surface state was favorable for the application of Zr-CNO on the cathode catalyst.

RRDE measurement was performed to estimate H_2O_2 generation under oxygen atmosphere. Figure 9 shows the polarization curves for the ORR of Zr-CNO treated at 1200°C with the rotation of the electrode at 400–3600 rpm and the H_2O_2 generation calculated using Eq. 2 as a function of the disk potential under oxygen saturated 0.1 M H_2SO_4 at 30°C. The potential of the Pt ring was held at 1.1 V vs RHE. As shown in Fig. 9, the ORR current increased with increasing electrode rotating speed at a lower potential. However, the diffusion-limited ORR current was not observed even at 400 rpm. As shown in Fig. 1b, the particle size of Zr-CNO was in the micrometer or submicrometer order. The particle size was too large to prepare the uniform thin catalyst layer on the disk electrode. In addition, the insufficient electrical contact between Zr-CNO and KB powders and the complex structure of the mixture of Zr-CNO and KB might interfere with the fluent oxygen diffusion on the surface of the active sites. The onset potential of the H_2O_2 generation was ca. 0.86 V at almost all rotating speeds. In addition, the ratio of the H_2O_2 generation drastically decreased with the increase in rotation speed. Further discussion is necessary considering the structure of the catalyst layer and the electrical contact between Zr-CNO and KB.

Surface characterization.— XPS was performed on $ZrC_{0.5}N_{0.5}$, Zr-CNO prepared at 1000, 1200, and 1400°C, and the ZrO_2 powders to analyze the surface oxidation state. Figure 10 shows the XPS of Zr 3d, O 1s, N 1s, and C 1s of (a) $ZrC_{0.5}N_{0.5}$, Zr-CNO prepared at (b) 1000, (c) 1200, and (d) 1400°C, and (e) ZrO_2. The value of the binding energy for Zr $3d_{5/2}$ reported for Zr^{4+} in pure zirconia was 182.26 eV.[30] However, the measured value of the binding energy for Zr $3d_{5/2}$ of ZrO_2 in this study (181.8 eV) was slightly smaller than that of the literature. We used 181.8 eV as the binding energy of Zr $3d_{5/2}$ of ZrO_2 in this study. In $ZrC_{0.5}N_{0.5}$, which was used as a starting material, two peaks were complicated in the Zr 3d spectra. One shifted lower than ZrO_2, and another existed higher. The binding energy of Zr $3d_{5/2}$ of ZrN was ca. 179.8 eV.[31] ZrC probably had a similar binding energy of Zr $3d_{5/2}$. Therefore, the lower Zr $3d_{5/2}$ peak, ca. 179.8 eV, was attributed to CN. The peaks attributed to ZrN (N 1s ZrN: 397.3 eV [32]) was observed in the N 1s spectra of $ZrC_{0.5}N_{0.5}$. In addition, in the C 1s spectra, there was a small peak at around 282 eV, which was responsible for ZrC (C 1s ZrC: 281.5 eV [33]) as well as free carbon (C 1s: 284.6 eV). These results also supported that Zr-CN existed near the surface of $ZrC_{0.5}N_{0.5}$. Another peak, Zr $3d_{5/2}$ of ca. 182.2 eV, was probably responsible for the hydroxide. The O 1s spectra of $ZrC_{0.5}N_{0.5}$ had a large shoulder around 531.6 eV. The peak due to hydroxide was positioned at 531.6 eV.[34] The Zr 3d and O 1s spectra of $ZrC_{0.5}N_{0.5}$ suggested that some of the oxides transformed to hydroxide on the surface. These results indicate that the surface of the $ZrC_{0.5}N_{0.5}$ powder was slightly oxidized in air, and the oxides partially transformed hydroxides on the surface.

In the O 1s spectra, the shoulder attributed to hydroxide at 531.6 eV decreased with the heat-treatment. In addition, the Zr 3d peak of the Zr-CNO powders shifted to a lower energy than that of $ZrC_{0.5}N_{0.5}$ and no N 1s peak was observed in the Zr-CNO. These results suggested that the surface of Zr-CNO was oxidized due to the partial oxidation, and the hydroxide on the surface transformed to oxide by the heat-treatment. However, a slight peak due to carbide in the C 1s spectra was observed in Zr-CNO, in particular, in Zr-CNO treated at 1200°C. This result indicated that the micro amount of carbon, which was responsible for carbidic carbon and not free carbon, existed near the oxidized surface.

Figure 11 shows the surface composition of Zr-CN, Zr-CNO, and the commercial ZrO_2 sample calculated using the relative response factor method. The carbon content contained the free carbon on the specimens. As shown in Fig. 11, the oxygen and carbon contents increased and decreased with the increase in heat-treatment tempera-

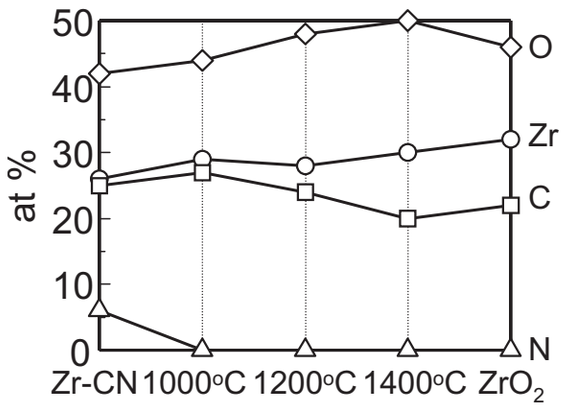

Figure 11. Surface composition of Zr-CN and Zr-CNOs by using relative response factor method.

ture, respectively. These results suggested that the amount of oxygen atoms replaced with carbon atoms increased with the increase in heat-treatment temperature, and the carbidic carbon atom might slightly exist on the surface of Zr-CNO.

The peaks attributed to Zr-CN were clearly observed in the XRD patterns of all Zr-CNOs, as shown in Fig. 2. Both XRD and XPS data suggested that Zr-CNO remained in the inner part of the particle, although the surface of Zr-CNO was oxidized. Considering that Zr-CNO with heat-treatment had some catalytic activity for the ORR, the surface that was identified as oxide by XPS was active for the ORR. In partially oxidized Ta-CN, the surface of the partially oxidized Ta-CN, which had some ORR activity, was oxidized as Ta_2O_5.[20] These results suggested that the highest oxidation state of metals on the surface of the partially oxidized metal CNs might be essential to have a definite catalytic activity for the ORR.

Correlation between catalytic activity for ORR and surface properties.— From our results, the partially oxidized $ZrC_{0.5}N_{0.5}$ powders have a clear catalytic activity for the ORR. The XPS analysis showed that the surface, which affects the catalytic activity for the ORR, was considerably oxidized. However, the completely oxidized and thermochemically stable monoclinic ZrO_2 had poor catalytic activity for the ORR. This is because the oxygen molecules hardly adsorb on the surface of the completely oxidized surface. The color of $ZrC_{0.5}N_{0.5}$ turned from deep purple to black through the partial oxidation. ZrO_2 with oxygen vacancies is black, whereas ZrO_2 with an ideal composition is white.[35] In this study, the partially oxidized specimens showed a black color. This result suggested that the growing oxide phase in Zr-CNO was ZrO_2 with oxygen vacancies. In addition, the oxide observed in Zr-CNO was not only monoclinic ZrO_2 but also tetragonal and cubic ZrO_2 in the XRD patterns of Zr-CNO. Pure ZrO_2 has three phases, with monoclinic, tetragonal, and cubic at atmospheric pressure. Pure zirconia with the monoclinic structure transforms near 1170°C into the tetragonal structure[36] and then near 2380°C into the cubic structure.[37] The tetragonal and cubic structure was stabilized with the introduction of oxygen vacancies by doping with several rare-earth oxides (MgO, Y_2O_3, etc.).[25,26,38] The introduction of vacancies by substituting some of the oxygen atoms with carbon and nitrogen atoms also stabilized the tetragonal and cubic structure.[25,26,39] The existence of the tetragonal or cubic phase suggested that vacancies were probably introduced by substituting the oxygen atoms with carbon and nitrogen atoms. According to the XPS analysis, no nitrogen was detected on the surface of all Zr-CNOs. Therefore, the residual carbidic carbon atom in the monoclinic ZrO_2 phase might mainly stabilize the tetragonal or cubic ZrO_2 phase through partial oxidation. Also, the XRD patterns of all Zr-CNOs indicated that vacancies might form due to mainly the residual carbon in the crystalline structure of Zr-CNO through the partial oxidation of $ZrC_{0.5}N_{0.5}$. Many researchers found that the surface defect sites were required to adsorb the oxygen molecules on the surface of the oxides.[40-44] The adsorption of oxygen molecules on the surface was required as the first step to proceed with the ORR. Therefore, the defects, such as vacancies and the remaining nitrogen and carbon atoms on the surface of Zr-CNO, might affect the activity of the ORR. However, more research is needed to clarify the active site for the ORR.

Conclusion

Partially oxidized $ZrC_{0.5}N_{0.5}$ was investigated as a nonprecious metal cathode for PEFCs. $ZrC_{0.5}N_{0.5}$ powder was heat-treated at 1000–1400°C under N_2 containing 2% H_2 and 0.25% O_2 gas to prepare Zr-CNO. The catalytic activity for the ORR significantly improved with partial oxidation. In particular, the onset potential of Zr-CNO prepared at 1200°C for the ORR reached 0.97 V vs RHE.

XRD and XPS data suggested that the surface of Zr-CNO was oxidized and $ZrC_{0.5}N_{0.5}$ remained in the inner part of Zr-CNO. The color of Zr-CNO was black, and the thermochemically unstable tetragonal and cubic ZrO_2 was observed in the XRD patterns of all Zr-CNOs, which suggests that the growing oxide phase had oxygen vacancies by substituting some of the oxygen atoms with nitrogen and carbon atoms. XPS indicated that the residual carbidic carbon atom in the monoclinic ZrO_2 phase might mainly stabilize the tetragonal or cubic ZrO_2 phase through partial oxidation. The defects, such as oxygen vacancies in Zr-CNO, might affect the catalytic activity for the ORR.

Acknowledgments

The authors thank ALMT Corporation for the supply of $ZrC_{0.5}N_{0.5}$ and Showa Denko for analyzing the specimens by SEM, XPS, and AES. The authors also thank the New Energy and Industrial Technology Development Organization (NEDO) for the financial support.

Yokohama National University assisted in meeting the publication costs of this article.

References

1. R. J. Jasinski, *Nature (London)*, **201**, 1212 (1964).
2. O. Contamin, C. Debiemme-Chouvy, M. Savy, and G. Scarbeck, *J. New Mater. Electrochem. Syst.*, **3**, 67 (2000).
3. P. Convert, C. Coutanceau, P. Crouigneau, F. Gloaguen, and C. Lamy, *J. Appl. Electrochem.*, **31**, 945 (2001).
4. H. Alt, H. Binder, and G. Sandstede, *J. Catal.*, **28**, 8 (1973).
5. P. Gouérec and M. Savy, *Electrochim. Acta*, **44**, 2653 (1999).
6. N. A. Vante and H. Tributsch, *Nature (London)*, **323**, 431 (1986).
7. H. Tributsch, *Catal. Today*, **39**, 177 (1997).
8. N. Alonso-Vante, I. V. Malakhov, S. G. Nikitenko, E. R. Savinova, and D. I. Kochubey, *Electrochim. Acta*, **47**, 3807 (2002).
9. D. Cao, A. Wieckowski, J. Inukai, and N. Alonso-Vante, *J. Electrochem. Soc.*, **153**, A869 (2006).
10. O. Solorza-Feria, K. Ellmer, M. Giersig, and N. Alonso-Vante, *Electrochim. Acta*, **39**, 1647 (1994).
11. T. J. Schmidt, U. A. Paulus, H. A. Gasteiger, N. Alonso-Vante, and R. J. Behm, *J. Electrochem. Soc.*, **147**, 2620 (2000).
12. I. V. Malakhov, S. G. Nikitenko, E. R. Savinova, D. I. Kochubey, and N. Alonso-Vante, *J. Phys. Chem. B*, **106**, 1670 (2002).
13. F. Dassenoy, W. Vogel, and N. Alonso-Vante, *J. Phys. Chem. B*, **106**, 12152 (2002).
14. J.-H. Kim, A. Ishihara, S. Mitsushima, N. Kamiya, and K. Ota, *Electrochim. Acta*, **52**, 2492 (2007).
15. K. Yato, S. Doi, A. Ishihara, S. Mitsushima, N. Kamiya, and K. Ota, *Suiso Enerugi Shisutemu*, **31**, 58 (2006).
16. A. Ishihara, S. Doi, S. Mitsushima, and K. Ota, *Electrochim. Acta*, **53**, 5442 (2008).
17. Y. Shibata, A. Ishihara, S. Mitsushima, N. Kamiya, and K. Ota, *Electrochem. Solid-State Lett.*, **10**, B43 (2007).
18. A. Ishihara, K. Lee, S. Doi, S. Mitsushima, N. Kamiya, M. Hara, K. Domen, K. Fukuda, and K. Ota, *Electrochem. Solid-State Lett.*, **8**, A201 (2005).
19. Y. Ohgi, A. Ishihara, Y. Shibata, S. Mitsushima, and K. Ota, *Chem. Lett.*, **37**, 608 (2008).
20. A. Ishihara, Y. Shibata, S. Mitsushima, and K. Ota, *J. Electrochem. Soc.*, **155**, B400 (2008).
21. Y. Liu, A. Ishihara, S. Mitsushima, N. Kamiya, and K. Ota, *J. Electrochem. Soc.*, **154**, B664 (2007).
22. Y. Maekawa, A. Ishihara, J.-H. Kim, S. Mitsushima, and K. Ota, *Electrochem. Solid-State Lett.*, **11**, B109 (2008).
23. A. Ishihara, S. Doi, Y. Liu, S. Mitsushima, N. Kamiya, and K. Ota, *Mater. Sci.*

Forum, **539–543**, 1379 (2007).
24. S. Doi, A. Ishihara, S. Mitsushima, N. Kamiya, and K. Ota, *J. Electrochem. Soc.*, **154**, B362 (2007).
25. M. Lerch and O. Rahaeuser, *J. Mater. Sci.*, **32**, 1357 (1997).
26. R. Collongues, J. C. Gilles, A. M. Lejus, M. Perez y Jorba, and D. Michel, *Mater. Res. Bull.*, **2**, 837 (1967).
27. U. A. Paulus, T. J. Schmidt, H. A. Gasteiger, and R. J. Behm, *J. Electroanal. Chem.*, **495**, 134 (2001).
28. S. Shimada, M. Johnsson, and S. Urbonaite, *Thermochim. Acta*, **419**, 143 (2004).
29. K. Kinoshita and J. A. S. Bett, *Carbon*, **11**, 403 (1973).
30. S. Tsunekawa, K. Asami, S. Ito, M. Yashima, and T. Sugimoto, *Appl. Surf. Sci.*, **252**, 1651 (2005).
31. S. M. Aouadi, P. Filip, and M. Debessai, *Surf. Coat. Technol.*, **187**, 177 (2004).
32. P. Prieto, L. Galan, and J. M. Sanz, *Phys. Rev. B*, **47**, 1613 (1993).
33. K. L. Håkansson, H. I. P. Johansson, and L. I. Johansson, *Phys. Rev. B*, **48**, 2623 (1993).
34. E. M. Moser, B. A. Keller, P. Lienemann, and P. Hug, *Fresenius' J. Anal. Chem.*, **346**, 255 (1993).
35. T. Arima, K. Moriyama, N. Gaja, H. Furuya, K. Idemitsu, and Y. Inagaki, *J. Nucl. Mater.*, **257**, 67 (1998).
36. G. Teufer, *Acta Crystallogr.*, **15**, 1187 (1962).
37. R. W. G. Wyckoff, *The Structure of Crystals*, 2nd ed., John Wiley & Sons, New York (1963).
38. S. Somiya, N. Yamamoto, and H. Yanagida, *Advances in Ceramics: Science and Technology of Zirconia III*, Vol. 24A, American Ceramic Society, Westerville, OH (1988).
39. S. Shimada, M. Nishisako, M. Inagaki, and K. Yamamoto, *J. Am. Ceram. Soc.*, **78**, 41 (1995).
40. J. M. Blaisdell and A. B. Kunz, *Phys. Rev. B*, **29**, 988 (1984).
41. C. Descorme, Y. Madier, and D. Duprez, *J. Catal.*, **196**, 167 (2000).
42. W. Göpel, *J. Vac. Sci. Technol.*, **15**, 1298 (1978).
43. A. L. Linsebigler, G. Lu, and J. T. Yates, Jr., *Chem. Rev. (Washington, D.C.)*, **95**, 735 (1995).
44. M. Witko and R. Tokarz-Sobieraj, *Catal. Today*, **91–92**, 171 (2004).